

# Wave propagation in one-dimensional optical quasiperiodic systems

J. M. Hollingworth and A. Vourdas

*Department of Electrical Engineering and Electronics, The University of Liverpool, Liverpool L69 3GJ, United Kingdom*

N. Backhouse

*Department of Mathematics, The University of Liverpool, Liverpool L69 3BX, United Kingdom*

(Received 19 March 2001; published 29 August 2001)

One-dimensional quasiperiodic optical systems are studied, using a Schrödinger-like equation with a potential  $V(x) = 2\lambda_1 \cos x + 2\lambda_2 \cos \alpha x$  as an approximation to the wave equation in the slowly-varying wave approximation. It is shown that small changes in the parameter  $\alpha$  produce major changes in the band structure of the system. For certain values of  $\alpha$ , the band structure consists of many “thin bands” and allows the possibility of dense multiplexing. The propagation of “noisy optical waves” that contain many frequencies with a thermal distribution is also studied with a thermodynamic model. Quantities like the thermodynamically averaged group velocity and the thermodynamically averaged inverse effective mass are introduced in order to quantify the complex relation between the frequency and wave vector in these systems.

DOI: 10.1103/PhysRevE.64.036611

PACS number(s): 42.65.Wi, 42.79.-e, 42.25.-p

## I. INTRODUCTION

It is well known that in solid state physics wave propagation in periodic structures leads to bands (intervals of allowed frequencies). In this context the waves describe electrons. This well known theory motivated recently the study of a similar phenomenon in the context of electromagnetic waves at microwave and optical frequencies propagating in structures with periodic refractive index (photonic crystals, e.g., [1]). In this context we get bands for the electromagnetic waves. In general, the periodicity in the refractive index of the material needs to be proportional to the wavelength. For optical frequencies very small periods are required, and very recently such materials have been fabricated.

From a mathematical point of view, this work is in the context of periodic systems that have been studied for many decades in various contexts: Partial differential equations, solid state Physics, Dynamical systems, etc. The solutions of the corresponding equations are based on the Floquet-Bloch theory.

Work on strictly periodic structures has recently been extended to quasiperiodic structures (e.g., [2]). Most of the existing work in this direction considers the discrete Schrödinger equation in the context of the tight binding Hamiltonian

$$H\psi = \psi(n+1) + \psi(n-1) + V(n)\psi(n) \quad (1)$$

(e.g., Fibonacci structures) for both one- and two-dimensional systems. This mathematical work motivated work on one- [3,4] and two-dimensional [5] photonic quasiperiodic crystals.

In this paper we consider the wave equation (in units where  $c = k_B = 1$ ):

$$[-\partial_x^2 + \partial_t^2]\psi = 0. \quad (2)$$

In the “slowly varying wave approximation,” we assume a wave of the form  $\exp(i\Omega t)\psi(x,t)$ , where  $\Omega$  is an “average frequency,” and Eq. (2) reduces to

$$[-\partial_x^2 - \Omega^2]\psi = -i2\Omega\partial_t\psi - \partial_t^2\psi. \quad (3)$$

In the slowly varying wave approximation, we assume that the second term on the right hand side of Eq. (3) is negligible in comparison to the first term. In this case, we get a Schrödinger-like equation. We use units in which  $2\Omega = c = k_B = 1$ , and all quantities are normalized accordingly.

In order to incorporate the varying refractive index, we include a potential  $V(x)$ . In this way we get the following equation written in the time-independent form

$$[-\partial_x^2 + V(x)]\psi(x) = \omega\psi(x). \quad (4)$$

In this paper we study explicitly the above eigenvalue equation. Its solutions can be used for the solution of the wave equation in the slowly varying wave approximation, which is first order with respect to time derivative; or even for the solution of the “full” wave equation, which is second order with respect to time derivative.

We consider the potential

$$V(x) = 2\lambda_1 \cos x + 2\lambda_2 \cos \alpha x, \quad (5)$$

which is periodic for rational values of  $\alpha$ , and quasiperiodic for irrational values of  $\alpha$ . A periodic refractive index will lead to a potential with many harmonics, and here for simplicity we consider only two harmonics with spatial angular frequencies  $q\gamma = 1$  and  $p\gamma = \alpha$  (where  $\gamma = 1/q$ ,  $\alpha = p/q$ , and  $p$  and  $q$  are coprime integers). A quasiperiodic refractive index can lead to a potential of the form of Eq. (5) with irrational  $\alpha$ . The quasiperiodic nature of the refractive index may be due to small fluctuations in the dielectric constants or widths of the several pieces that constitute the stack, as studied in Ref. [4].

We study the spectrum of Eq. (4) and show that for rational values of  $\alpha$  (in which case we have bands according to Bloch theory), small changes in the parameter  $\alpha$  produce major changes in the band structure of the system. When  $\alpha = p/q$ , where  $p$  and  $q$  are coprime integers, and  $q$  is large, the

band structure consists of many very thin bands, which can be used for the transmission of many different optical signals (dense multiplexing). There is an increasing demand for multiplexing in modern communications systems. Our results demonstrate that suitable values of  $\alpha$  can achieve ultradense multiplexing, with important implications for optical technology. We note that the sensitivity of our results to the values of  $\alpha$  is similar to the ‘‘anomalies’’ reported in [4].

In practice, even a ‘‘monochromatic’’ optical signal will contain a distribution of frequencies due to noise. In order to model this, we assume a thermal distribution of frequencies, and study the thermodynamics of this system. It is shown that small changes in the parameter  $\alpha$  produce major changes in the values of the thermodynamic quantities of the system. The concepts of thermodynamically averaged group velocity and thermodynamically averaged inverse effective mass are introduced in order to quantify the complex relation between the frequency and wave vector.

## II. BACKGROUND FORMALISM

We consider Eq. (4) with the potential  $V(x)$  of Eq. (5). The potential is periodic for rational values of  $\alpha = p/q$  (where  $p$  and  $q$  are coprime integers) with period  $2\pi q$ ; and quasiperiodic for irrational values of  $\alpha$ . It is seen that for rational  $\alpha$ , very small changes in the value of  $\alpha$  can produce very large changes in the period. For example, as  $\alpha$  changes from  $1/2$  to  $10/21$  the period changes from  $4\pi$  to  $42\pi$ . Below we will present results for various quantities and for various rational values of  $\alpha$  very close to a certain rational  $\alpha_0$ . Irrational values of  $\alpha$  will also be studied through the continued fraction expansion:

$$\alpha = \alpha_0 + \frac{1}{\alpha_1 + \frac{1}{\alpha_2 + \dots}}, \quad (6)$$

where

$$p_{n+1} = \alpha_{n+1} p_n + p_{n-1}, \quad (7)$$

$$q_{n+1} = \alpha_{n+1} q_n + q_{n-1}, \quad (8)$$

and  $p_{-1} = 1, q_{-1} = 0, p_0 = \alpha_0, q_0 = 1$ . The sequence of convergents

$$\frac{p_1}{q_1}, \frac{p_2}{q_2}, \dots \rightarrow \alpha \quad (9)$$

tends to  $\alpha$  in an oscillatory manner.

For potentials with period  $2\pi q$ , use of Bloch’s theorem leads to the solution

$$\psi_k(x) = \exp\left(\frac{ikx}{q}\right) \psi_0(x), \quad (10)$$

where  $\psi_0(x)$  is a periodic function with period  $2\pi q$  that can be expanded as

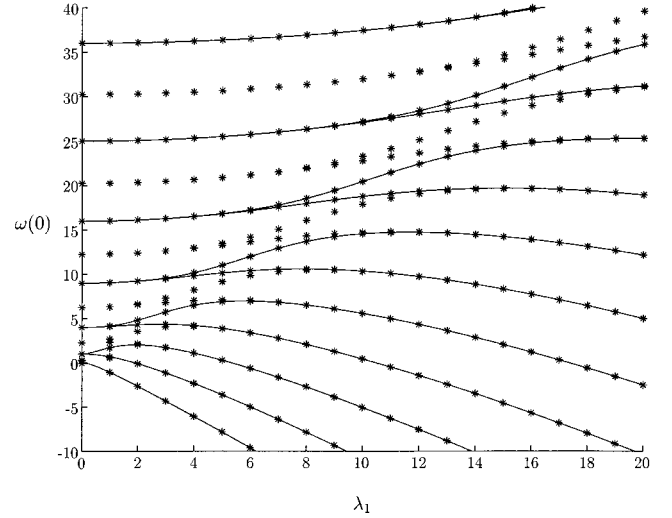


FIG. 1. The eigenvalues  $\omega(k=0)$  against  $\lambda_1$  for the potential  $V(x) = 2\lambda_1 \cos x + 2\lambda_2 \cos(x/2)$  with  $\lambda_2 = 0$  (solid lines) and  $\lambda_2 = 0.1$  (star lines). We use units in which  $2\Omega = c = k_B = 1$ .

$$\psi_0(x) = \sum_{n=-\infty}^{\infty} a_n e^{inx/q}. \quad (11)$$

$\psi_k(x)$  is a quasiperiodic function

$$\psi_k(x + 2\pi q) = \psi_k(x) e^{i2\pi k}, \quad (12)$$

where  $k$  takes values from 0 to 1. Combining Eqs. (10) and (11), and inserting into Eq. (4), we get the matrix equation

$$A_{nm} a_m = \omega(k) a_n, \quad (13)$$

where

$$A_{nm} = \left(\frac{n+k}{q}\right)^2 \delta(n, m) + \lambda_1 \delta(n-q, m) + \lambda_1 \delta(n+q, m) + \lambda_2 \delta(n-p, m) + \lambda_2 \delta(n+p, m), \quad (14)$$

and  $\delta(n, m)$  is Kronecker’s delta,  $\omega(k)$  is a periodic function of  $k$  with period 1.

We have truncated the infinite matrices by allowing the indices to take values from  $-N_{max}$  to  $N_{max}$  and have evaluated numerically the eigenvectors and eigenvalues. In all our numerical results we used  $N_{max} = 10q$ . In Fig. 1 we show the eigenvalues against  $\lambda_1$ , for  $V(x) = 2\lambda_1 \cos x + 2\lambda_2 \cos(x/2)$ ,  $k = 0$ , and for  $\lambda_2 = 0$  (solid lines);  $\lambda_2 = 0.1$  (star lines). In the latter case the spectrum is denser due to the fact that the period is larger. This is true even for very small values of  $\lambda_2$ , and it is seen that small perturbations [by the term  $2\lambda_2 \cos(x/2)$ ] produce major changes in the spectrum. As the amplitude of the potential increases (by increasing  $\lambda_1$ ), we get splitting of the eigenvalues.

## III. BANDS AND MULTIPLEXING

In this section we show that small changes in the parameter  $\alpha$  of the potential produce major changes in the band structure of the model. We study two aspects of the general

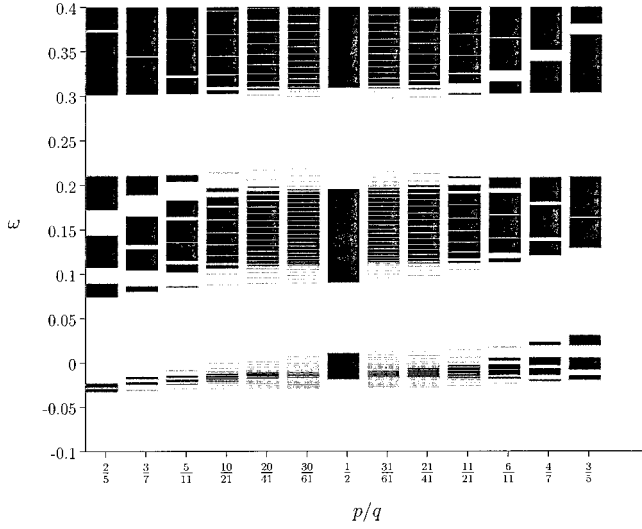


FIG. 2. The bands for the potential  $2\lambda_1 \cos x + 2\lambda_2 \cos(px/q)$  with  $\lambda_1=0.05$ ,  $\lambda_2=0.05$ , and various values of  $p/q$  close to  $1/2$ . We use units in which  $2\Omega = c = k_B = 1$ .

problem. In Sec. III A, we consider numbers  $p_n/q_n$  very close to  $1/2$ , and show that the results are very sensitive to the exact value  $p_n/q_n$ . In Sec. III B, the numbers  $p_n/q_n$  are convergents of an infinite continued fraction, and we study the spectrum. We show that nesting of bands takes place that in our context can be used for dense multiplexing.

### A. Sensitive dependence of bands on $\alpha$

In the previous section we have calculated the eigenvalues  $\omega(k)$  as a function of  $k$ . The bands are the allowed values of frequency (presented in black in the figures). For later purposes, we stress that the endpoints of the band are included in the band, i.e., mathematically the bands are closed intervals. In Fig. 2 we present the lowest part of the bands for the potential

$$V(x) = 2\lambda_1 \cos x + 2\lambda_2 \cos\left(\frac{px}{q}\right), \quad (15)$$

with  $\lambda_1=0.05$ ,  $\lambda_2=0.05$ , and for various values of  $p/q$  that are very close to  $1/2$ . In Fig. 3 we present the bands for the same potential with  $\lambda_1=0.2$ ,  $\lambda_2=0.2$ . It is seen that the band structure is complicated and is very sensitive to the value of  $\alpha$ .

### B. Nesting of bands and dense multiplexing

In order to explain this band structure we first consider the simple case  $\lambda_1=0$  and  $\lambda_2 \rightarrow 0$ . In this case the frequency spectrum is  $\omega_n = [(n+k)/q]^2$  and we get bands from  $(n/q)^2$  to  $[(n+1)/q]^2$ , which for a very small potential are separated by a very small gap  $g \approx 0$ . As the potential increases, the gap increases and the band becomes  $[(n/q)^2 + g_n, \{(n+1)/q\}^2 - g_{n+1}]$ , where the  $g_i$  are gaps. In the case of a sequence of convergents corresponding to a given  $\alpha$ , the period of the problem increases in the  $m$ th step from  $2\pi q_m$  to  $2\pi q_{m+1}$ , where  $q_m$  and  $q_{m+1}$  are related as described in

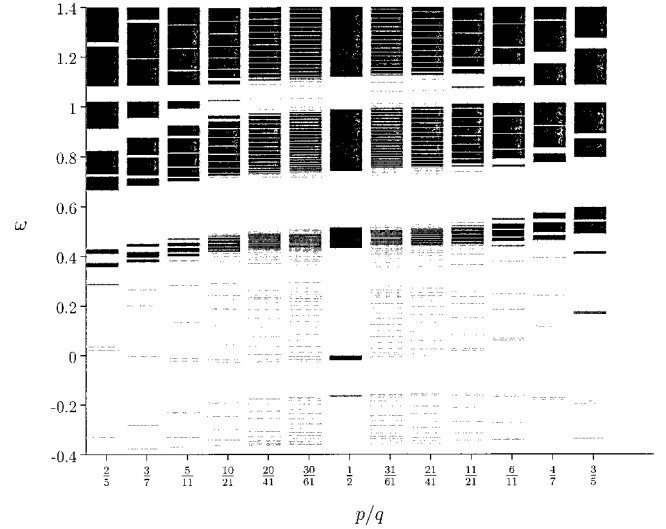


FIG. 3. The bands for the potential  $2\lambda_1 \cos x + 2\lambda_2 \cos(px/q)$  with  $\lambda_1=0.2$ ,  $\lambda_2=0.2$ , and various values of  $p/q$  close to  $1/2$ . We use units in which  $2\Omega = c = k_B = 1$ .

Eq. (8). Due to this increase in the period, the spectrum becomes denser and each band splits into more bands. For example, for  $\alpha_m$  large, so that Eq. (8) gives  $q_{m+1} \approx \alpha_{m+1} q_m$ , the band

$$\left[ \left( \frac{1}{q_m} \right)^2 + g_1, \left( \frac{2}{q_m} \right)^2 - g_2 \right] \quad (16)$$

will split into many bands, where the first one is

$$\left[ \left( \frac{\alpha_{m+1}}{q_{m+1}} \right)^2 + g_1, \left( \frac{\alpha_{m+1} + 1}{q_{m+1}} \right)^2 - g_{1,1} \right], \quad (17)$$

the second one is

$$\left[ \left( \frac{\alpha_{m+1} + 1}{q_{m+1}} \right)^2 + g_{1,1}, \left( \frac{\alpha_{m+1} + 2}{q_{m+1}} \right)^2 - g_{1,2} \right], \quad (18)$$

etc. This shows the process of band splitting and nesting. Rigorously speaking, nesting occurs only when  $q_{m+1}$  is an integer multiple of  $q_m$  ( $q_{m+1} = \alpha_{m+1} q_m$ ). In the case  $q_{m+1} = \alpha_{m+1} q_m + q_{m-1}$ , which really occurs here, a small number of the new bands might overlap previous band gaps. But the majority of them are clearly nested within the previous ones. In Fig. 4 we demonstrate nesting for the example of Eq. (15) with  $p/q=1/5$  and  $p/q=1/(5+1/7)=7/36$ . We have checked that for large values of  $\alpha_m$ , we get a very clear nesting while for smaller values the nesting is not complete.

At each step the density of bands (i.e., the number of bands per original band) is greater than 1. The lowest density occurs when all  $\alpha_m=1$  (Fibonacci sequence) which is known to lead to a density factor of the Golden ratio. In the case of large  $\alpha_m$  considered here, the density will be much greater than the Golden ratio.

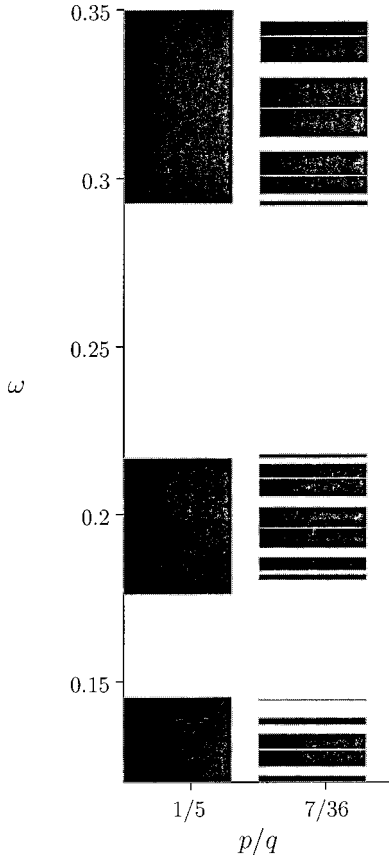


FIG. 4. The bands for the potential  $2\lambda_1 \cos x + 2\lambda_2 \cos(px/q)$  with  $\lambda_1=0.05$ ,  $\lambda_2=0.05$ , and  $p/q=1/5, 1/(5+1/7)=7/36$ . The nesting is clearly seen. We use units in which  $2\Omega=c=k_B=1$ .

#### IV. NOISY OPTICAL SIGNALS WITH A THERMAL DISTRIBUTION

Optical signals in realistic systems will be noisy. This is due to noise in the laser source, impurities, external vibrations, etc. In this section we model noisy optical signals assuming a thermal distribution. We study various thermodynamic quantities and show that small changes in the parameter  $\alpha$  produce major changes in the thermodynamics of the system.

The partition function is defined as

$$Z(\beta, k) = \sum_{N=0}^{\infty} \exp(-\beta \omega_N), \quad (19)$$

where  $\beta=T^{-1}$  is the inverse temperature that quantifies the amount of noise, and  $\omega_N$  are the eigenfrequencies. We also define the probabilities  $s_N=Z^{-1} \exp(-\beta \omega_N)$ . The free energy is defined by

$$F(\beta, k) = \frac{-1}{\beta} \ln Z, \quad (20)$$

the average frequency

$$\langle \omega \rangle(\beta, k) \equiv \sum_{N=0}^{\infty} \omega_N s_N = -\partial_{\beta} \ln Z, \quad (21)$$

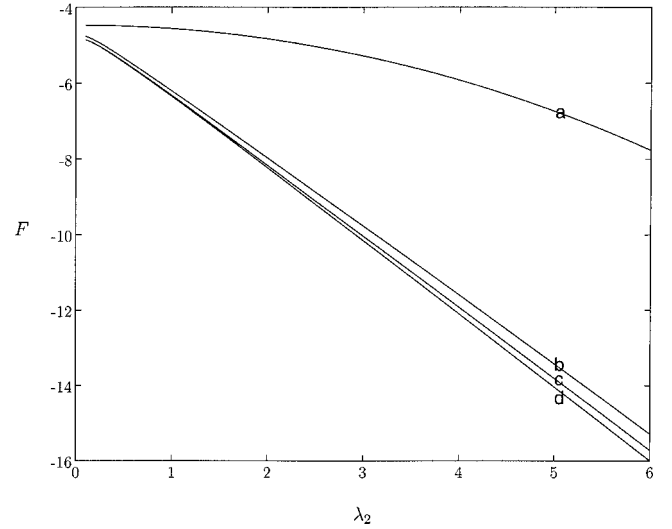


FIG. 5. Free energy against  $\lambda_2$  for the potential  $2\lambda_1 \cos x + 2\lambda_2 \cos(px/q)$  with  $\lambda_1=3$ ,  $\beta=5$  and (a)  $p/q=1/2$ , (b)  $p/q=4/7$ , (c)  $p/q=6/11$ , (d)  $p/q=3/7, 5/11, 10/21, 11/21$  (for these four values of  $p/q$ , the curves are practically identical). We use units in which  $2\Omega=c=k_B=1$ .

and the entropy

$$S(\beta, k) \equiv -\sum_{N=0}^{\infty} s_N \ln s_N = -\ln Z + \beta \langle \omega \rangle = (1 - \beta \partial_{\beta}) \ln Z. \quad (22)$$

In the context of wave propagation in quasiperiodic structures  $\langle \omega \rangle(\beta, k)$  shows the complicated temperature-dependent (i.e., noise dependent) relation between the frequency  $\langle \omega \rangle$  and the wave vector  $k$ . The entropy  $S(\beta, k)$  quantifies the uncertainty in the frequency due to noise.

In Figs. 5–7 we plot these quantities for various values of

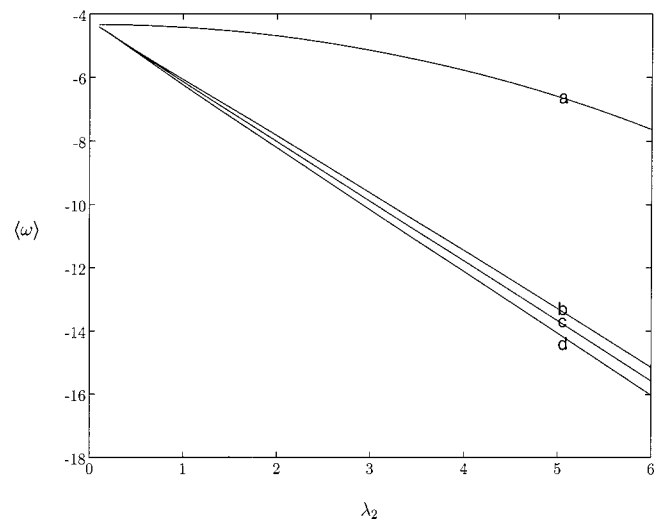


FIG. 6. Average frequency against  $\lambda_2$  for the potential  $2\lambda_1 \cos x + 2\lambda_2 \cos(px/q)$  with  $\lambda_1=3$ ,  $\beta=5$ , and (a)  $p/q=1/2$ , (b)  $p/q=4/7$ , (c)  $p/q=6/11$ , (d)  $p/q=3/7, 5/11, 10/21, 11/21$  (for these four values of  $p/q$ , the curves are practically identical). We use units in which  $2\Omega=c=k_B=1$ .

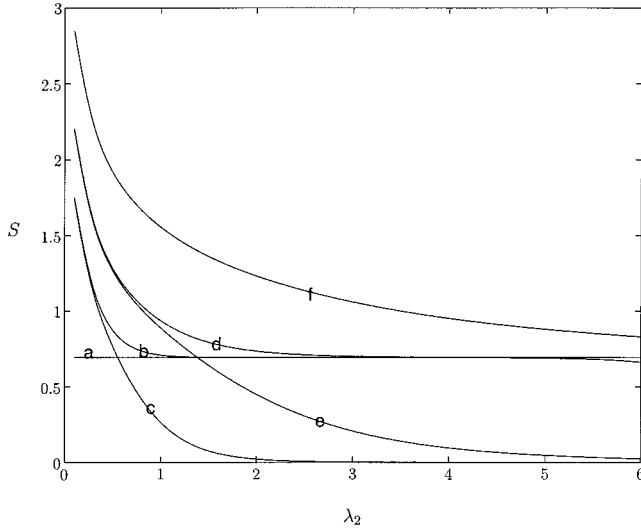


FIG. 7. Entropy against  $\lambda_2$  for the potential  $2\lambda_1 \cos x + 2\lambda_2 \cos(px/q)$  with  $\lambda_1=3$ ,  $\beta=5$  and (a)  $p/q=1/2$ , (b)  $p/q=4/7$ , (c)  $p/q=3/7$ , (d)  $p/q=6/11$ , (e)  $p/q=5/11$ , (f)  $p/q=10/21, 11/21$  (for these two values of  $p/q$ , the curves are practically identical). We use units in which  $2\Omega=c=k_B=1$ .

$p/q$  that are very close to  $1/2$ , for  $\lambda_1=3$ , and over ranges of  $\lambda_2$ . It is seen that all the thermodynamic quantities are very sensitive to  $p/q$ . This is because the spectrum is denser for larger denominators  $q$ . We also note that as  $\lambda_2$  increases, the entropy  $S$  tends either to zero or to  $\ln 2$ , depending on  $p/q$ . This is because the potential function  $V(x)$ , as defined in Eq. (15), has, respectively, either one or two global minima in each period.

### A. Average group velocity

The thermodynamically averaged group velocity is given by

$$v_{av} \equiv \left\langle \frac{\partial \omega}{\partial k} \right\rangle = \sum_N \frac{\partial \omega_N}{\partial k} s_N = \frac{-1}{\beta} \partial_k \ln Z. \quad (23)$$

For simplicity we will refer to this as the average velocity,  $\omega(k)$  is a periodic function of  $k$  with period 1, and this implies that all  $\partial \omega_N / \partial k$  are periodic with period 1. Consequently  $v_{av}$  is a periodic function of  $k$ .

In Fig. 8, we present the average velocity against  $k$  for  $\beta=500$  and for the potential  $2\lambda_1 \cos x + 2\lambda_2 \cos(px/q)$  with  $\lambda_1=0.05$ ,  $\lambda_2=0.05$  and various values of  $p/q$  close to  $1/2$ . It is seen that for very low temperatures (large  $\beta$ ) the average velocity is nonzero and is very sensitive to the exact value of  $p/q$ . In Fig. 9 we present the average velocity against  $\beta$  for  $k=0.3$  and for the same potential. It is seen that at higher temperatures the average velocity is zero.

### B. Effective mass

We introduce the concept of thermodynamically averaged inverse effective mass for the propagating waves as

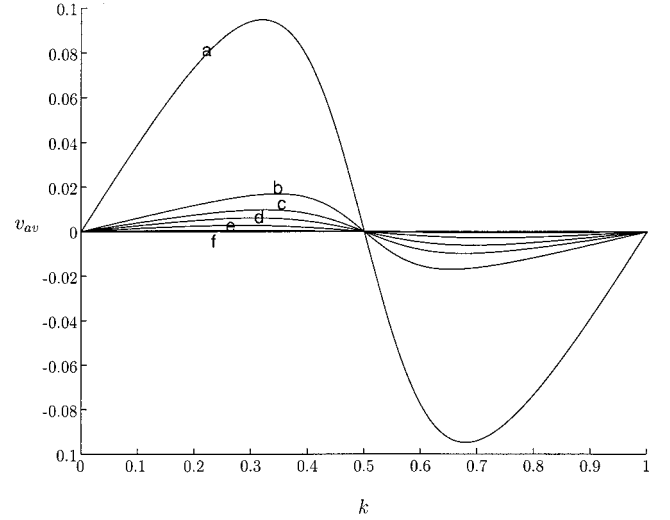


FIG. 8. Average velocity against  $k$  for the potential  $2\lambda_1 \cos x + 2\lambda_2 \cos(px/q)$  with  $\beta=500$ ,  $\lambda_1=0.05$ ,  $\lambda_2=0.05$  and (a)  $p/q=1/2$ , (b)  $p/q=3/5$ , (c)  $p/q=2/5$ , (d)  $p/q=4/7$ , (e)  $p/q=3/7$ , (f)  $p/q=5/11, 6/11, 10/21, 11/21, 20/41, 21/41, 30/61, 31/61$  (for these eight values of  $p/q$ , the curves are practically identical). We use units in which  $2\Omega=c=k_B=1$ .

$$[m_1(k, \beta)]^{-1} = \frac{\partial}{\partial k} \left\langle \frac{\partial \omega}{\partial k} \right\rangle = \frac{\partial v_{av}}{\partial k} = \frac{-1}{\beta} \partial_k^2 \ln Z \quad (24)$$

or as

$$[m_2(k, \beta)]^{-1} = \left\langle \frac{\partial^2 \omega}{\partial k^2} \right\rangle. \quad (25)$$

In the first case we differentiate with respect to  $k$  the average velocity (which, as explained above is the thermodynamically averaged group velocity). In the second case we calcu-

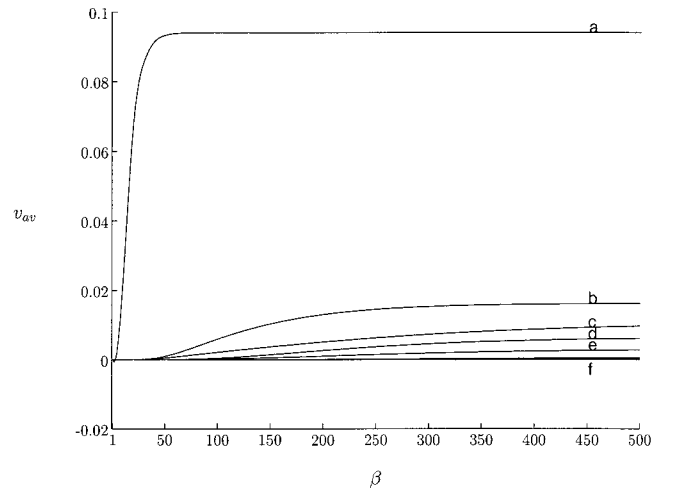


FIG. 9. Average velocity against  $\beta$  for the potential  $2\lambda_1 \cos x + 2\lambda_2 \cos(px/q)$  with  $k=0.3$ ,  $\lambda_1=0.05$ ,  $\lambda_2=0.05$  and (a)  $p/q=1/2$ , (b)  $p/q=3/5$ , (c)  $p/q=2/5$ , (d)  $p/q=4/7$ , (e)  $p/q=3/7$ , (f)  $p/q=5/11, 6/11, 10/21, 11/21, 20/41, 21/41, 30/61, 31/61$  (for these eight values of  $p/q$ , the curves are practically identical). We use units in which  $2\Omega=c=k_B=1$ .

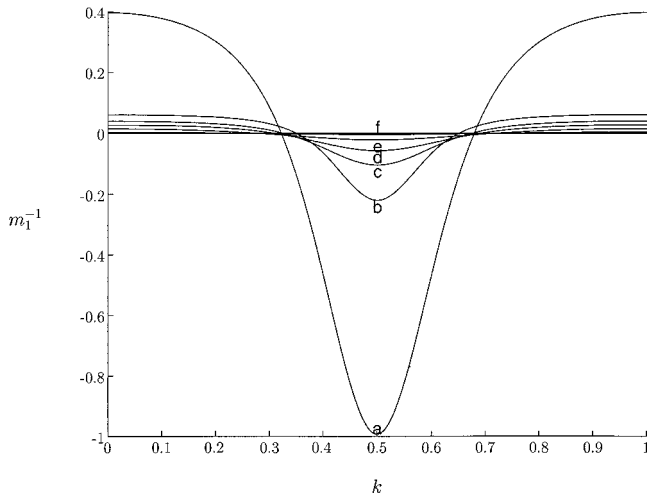


FIG. 10. Inverse effective mass  $1/m_1(k, \beta)$  against  $k$  for  $\beta = 500$  and for the potential  $2\lambda_1 \cos x + 2\lambda_2 \cos(px/q)$  with  $\lambda_1 = 0.05$ ,  $\lambda_2 = 0.05$ , and (a)  $p/q = 1/2$ , (b)  $p/q = 2/5$ , (c)  $p/q = 3/5$ , (d)  $p/q = 4/7$ , (e)  $p/q = 3/7$ , (f)  $p/q = 5/11, 6/11, 10/21, 11/21, 20/41, 21/41, 30/61, 31/61$  (for these eight values of  $p/q$ , the curves are practically identical). We use units in which  $2\Omega = c = k_B = 1$ .

late the thermodynamically averaged value of the second derivative  $\partial^2 \omega / \partial k^2$ . These two quantities are similar, and the numerical results confirm that at very low temperatures or for high values of the coupling constants  $\lambda_1, \lambda_2$  they are almost equal. But at higher temperatures and for low values of the coupling constants they are different. Like the quantities introduced in the previous subsection, they also quantify the complicated effect of the potential on the propagating waves.

Straightforward differentiation of the results presented in Fig. 8 gives  $1/m_1$  (Fig. 10). We have also calculated numerically  $1/m_2$ , and present results in Fig. 11. It is seen that the inverse effective masses  $[m_1(k, \beta)]^{-1}$  and  $[m_2(k, \beta)]^{-1}$  become zero and also take negative values for certain values of  $k$ . These results for  $1/m_1$  are anticipated from the general mathematical properties of  $v_{av}$ . Periodic functions like  $v_{av}$  that are continuous and differentiable everywhere, have maxima and minima where the slope is zero and, which correspond to the zeros of  $1/m_1$ . They also have regions of negative slope that correspond to the negative values of  $1/m_1$ . In a similar way we can explain the behavior of  $1/m_2$ .

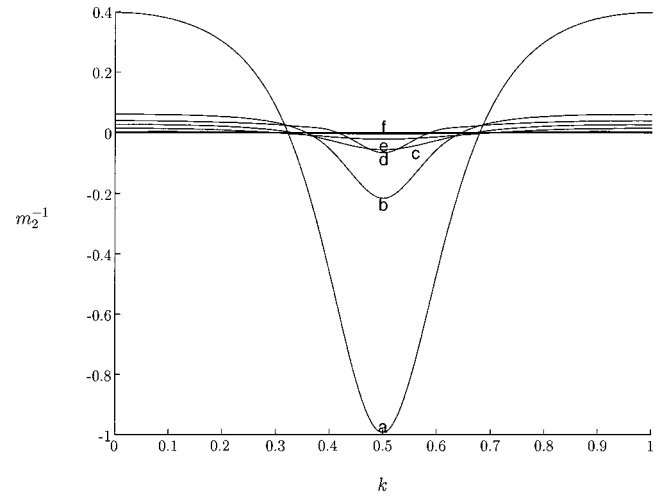


FIG. 11. Inverse effective mass  $1/m_2(k, \beta)$  against  $k$  for  $\beta = 500$  and for the potential  $2\lambda_1 \cos x + 2\lambda_2 \cos(px/q)$  with  $\lambda_1 = 0.05$ ,  $\lambda_2 = 0.05$ , and (a)  $p/q = 1/2$ , (b)  $p/q = 2/5$ , (c)  $p/q = 3/5$ , (d)  $p/q = 4/7$ , (e)  $p/q = 3/7$ , (f)  $p/q = 5/11, 6/11, 10/21, 11/21, 20/41, 21/41, 30/61, 31/61$  (for these eight values of  $p/q$ , the curves are practically identical). We use units in which  $2\Omega = c = k_B = 1$ .

## V. DISCUSSION

We have considered optical wave propagation in quasi-periodic systems in the slowly varying wave approximation, modeled with Eq. (4) with the potential (5), which can be periodic or quasiperiodic. When  $\alpha$  is rational, the potential is periodic and we have demonstrated that the bands split as the denominator of  $\alpha$  increases. This shows that suitable values of  $\alpha$  can achieve ultradense multiplexing. The sensitivity of various quantities to small changes in the value of  $\alpha$  has been studied, and can be used to define the tolerances that these system can have while still preserving the dense multiplexing.

We have modeled noisy signals that occur in practice with a thermal distribution of frequencies. We have studied the thermodynamics of these signals and calculated the complex relationship between the frequency  $\langle \omega \rangle$  and the wave vector  $k$ . This has been quantified with quantities like the thermodynamically averaged group velocity of Eq. (23) and the effective masses of Eqs. (24) and (25).

From a practical point of view, the work is a contribution to the currently “hot” problem of ultradense multiplexing in optical communications. We believe that photonic quasicrystal fibers may be used for ultradense multiplexing.

[1] E. Yablonovitch, *J. Mod. Opt.* **41**, 173 (1994); J.D. Joannopoulos, P.R. Villeneuve, and S. Fan, *Nature (London)* **386**, 143 (1997).  
 [2] *Number Theory and Physics*, edited by J.-M. Luck, P. Moussa, and M. Waldschmidt (Springer, Berlin, 1990); *From Number Theory to Physics*, edited by M. Waldschmidt, P. Moussa, J.-M. Luck, and C. Itzykson (Springer, Berlin, 1992); M. Senechal, *Quasicrystals and Geometry* (Cambridge University Press, Cambridge, 1995); *Quasicrystals and Discrete Geom-*

*etry*, edited by J. Patera (AMS, Rhode Island, 1998).

[3] W. Gellermann, M. Kohmoto, B. Sutherland, and P.C. Taylor, *Phys. Rev. Lett.* **72**, 633 (1994); T. Hattori, N. Tsurumachi, S. Kawato, and H. Nakatsuka, *Phys. Rev. B* **50**, R4220 (1994); R. Pelster, V. Gasparian, and G. Nimtz, *Phys. Rev. E* **55**, 7645 (1997); R.W. Peng, M. Wang, A. Hu, S.S. Jiang, G.J. Jin, and D. Feng, *Phys. Rev. B* **57**, 1544 (1998); C. Sibilia, P. Masciulli, and M. Bertolotti, *Pure Appl. Opt.* **7**, 383 (1998); C. Sibilia, I.S. Nefedov, M. Scalora, and M. Bertolotti, *J. Opt. Soc. Am. B*

- 15**, 1947 (1998); M.S. Vasconcelos, E.L. Albuquerque, and A.M. Mariz; *J. Phys.: Condens. Matter* **10**, 5839 (1998); C. Sibilila, M. Scalora, M. Centini, M. Bertolotti, M.J. Bloemer, and C.M. Bowden; *J. Opt. A, Pure Appl. Opt.* **1**, 490 (1999).
- [4] B.A. van Tiggelen and A. Tip, *J. Phys. I* **1**, 1145 (1991); R. Sprik, B.A. van Tiggelen, and A. Lagendijk, *Europhys. Lett.* **35**, 265 (1996); A. Moroz and A. Tip, *J. Phys.: Condens. Matter* **11**, 2503 (1999); A. Tip, A. Moroz, and J.M. Combes, *J. Phys. A* **33**, 6223 (2000).
- [5] Y.S. Chan, C.T. Chan, and Z.Y. Liu, *Phys. Rev. Lett.* **80**, 956 (1998); S.S.M. Cheng, L.-M. Li, C.T. Chan, and Z.Q. Zhang, *Phys. Rev. B* **59**, 4091 (1999); C. Jin, B. Cheng, B. Man, Z. Li, D. Zhang, S. Ban, and B. Sun, *Appl. Phys. Lett.* **75**, 1848 (1999); M.E. Zoorob, M.D.B. Charlton, G.J. Parker, J.J. Baumberg, and M.C. Netti, *Nature (London)* **404**, 740 (2000); C. Jin, B. Cheng, B. Man, Z. Li, and D. Zhang, *Phys. Rev. B* **61**, 10 762 (2000); M.A. Kaliteevski, S. Brand, R.A. Abram, T.F. Krauss, R. de la Rue, and P. Millar, *J. Mod. Opt.* **47**, 1771 (2000); M.A. Kaliteevski, S. Brand, R.A. Abram, T.F. Krauss, R. de la Rue, and P. Millar, *ibid.* **48**, 9 (2001).